



## FLEXURAL PROPERTIES OF BOLTED WIDE FLANGE COLUMN SPLICES

F. Tork Ladani<sup>(1)</sup>, G. MacRae<sup>(2)</sup>, G. Chase<sup>(3)</sup>, G. C. Clifton<sup>(4)</sup>

<sup>(1)</sup> PhD Student, University of Canterbury, [Fahimeh.torkladani@pg.canterbury.ac.nz](mailto:Fahimeh.torkladani@pg.canterbury.ac.nz)

<sup>(2)</sup> A/Professor, University of Canterbury, [Gregory.macrae@canterbury.ac.nz](mailto:Gregory.macrae@canterbury.ac.nz)

<sup>(3)</sup> Distinguished Professor, University of Canterbury, [Geoff.chase@canterbury.ac.nz](mailto:Geoff.chase@canterbury.ac.nz)

<sup>(4)</sup> A/Professor, University of Auckland, [c.clifton@canterbury.ac.nz](mailto:c.clifton@canterbury.ac.nz)

### **Abstract**

Current standards for designing steel structures indicate that column splices, as part of moment frames, should develop a certain level of plastic moment capacity (ranging from 30 to 100 percent) of the smaller section of the connection. However, there is not any provision for the ductility or stiffness requirements of these connections. While welded splices can be considered as rigid connections, bolted splices are likely to rotate in an earthquake event.

In this paper, experimental tests on hysteretic flexural behavior of bolted column splice connections about their major axes are presented. The tests are conducted in order to investigate strength, stiffness and ductility properties of splices designed for different strength capacities. Commonly used design procedures assume that flange cover plates transfer moment while web splices transfer shear force. To characterize the force distribution between flange and web splices, web splices are eliminated in one specimen.

A component-based connection model is developed. The key parameters are slippage, bolt shear deformation, splice plate deformation and ovalization of bolt holes. The models show good agreement with the experimental results.

Also, it is shown that splice capacities during pure flexural testing with bending about the strong axis was, in all cases, about 50% greater than the design capacities. This may be partly attributed to the overstrength of the component material. The presence of the web plate did not change the flexural strength but it did result in web splice damage.

*Keywords: wide flange section, flexural properties, bolted connections, column splices*

## 1. Introduction

Past earthquakes have demonstrated the vulnerability of connections in steel frames. Although beam-column connections have received a lot of research attention, column splice performance is not well-understood.

Column splices are required to develop certain amount of axial, shear and moment capacity as part of a gravity or moment frame. But the values differ in different standards. In US standards, the steel seismic design provisions, AISC 341-10 [1] clauses E2.6g and E3-6g, stipulate design flexural capacity of column splices in special and intermediate frames to be at least equal to the flexural strength of the smaller column. The shear strength of the splice is prescribed to satisfy the demand associated with the flexural hinging at both ends of the column assuming double curvature deflection. Current NZS 3404 design specifications [2] for column splices, in frames required to resist significant seismic forces (i.e. Category 1 and 2 frames), require the connection to provide 50% of the reduced flexural design strength of the smaller column (i.e.  $\phi M_p$ ), as well as 25% of its design shear capacity.

Welding and bolting are two common methods of fabricating splices. There are few experimental research studies addressing shear and flexural performance of column splices. While welded splices act as rigid connections, rotation is very likely to occur in bolted splices. Currently, there is not any specific provision for the required stiffness of splices for an earthquake event, which may affect overall frame performance. If splices are strong enough to carry the demand, but not sufficiently stiff, they may exhibit large deformations at a certain level of strength which could be detrimental.

Bruneau et al. [3] performed moment tests on partial and full penetration butt welded splices in heavy steel sections subjected to pure bending. According to their report, partial penetration joints are likely to have brittle fracture especially in thicker flanges, whereas full penetration joints develop ductile behavior. Stillmaker et al. [4] conducted analytical and experimental studies on partially welded column splices and proposed a method for seismic design of partially welded column splices.

Edwards et al. [5] performed monotonic pure moment experiments on major and minor axis behavior of welded-bolted splices in H-section columns. The connections tested are not a common way of splicing in modern practice. Douty et al. [6] studied the performance of beam splices under monotonic pure moment loading as part of beam-column connection investigations. They observed that the maximum moment capacity was equal to, or greater than the theoretical plastic moment of the gross section in all cases. Beedle et al. [7] reported two moment experiments conducted at University of Cambridge in 1958 on beam splices. One of the specimens was designed as a riveted full plastic moment splice, where rivets were substituted with bolts. The other was connected by half as many bolts. It was shown that the weaker connection could also develop the full assembly plastic capacity at the expense of larger rotations.

The literature provides only an overview of splice strength but it does not provide a methodical approach to investigate stiffness and ductility characteristics. Moreover, the connections tested in the literature are generally for beams with the same section size either side of the splice. Findings and component models developed from such tests may therefore not be relevant to column splices with different section sizes. Also, the monotonic performance of the connections may be different from their cyclic behavior.

This paper summarizes the results of several experiments and analyses to address:

- The flexural performance of splices designed for various levels of design actions about the major axis
- The contribution of web cover plate in carrying major axis moment
- A simple approach to predict bolted column splice behavior

## 2. Methodology

### 2.1 Experimental program

The column members used in this study were of Grade 300 steel, 310UC158 and 310UC118 wide flange sections spliced together. The 310UC158 is the largest universal column section available. Therefore, the splice connections provide real scale test results. Bolts were Grade 8.8 M20 bolts.

Three tests were conducted to study the connection bending performance. The connections had two different strength capacities, and were subjected to pure moment about their major axis. The web splice was eliminated in one of the connections to investigate the effect of the web splice in bending.

Specimen #1 was approximately designed for the minimum design actions prescribed in the NZ Steel Structure Standard NZS3404 for ductile moment frames. These are 50% of the reduced moment capacity of the smaller section in splice and 25% of reduced shear capacity. Specimen #2 has the same flange splice components but was not spliced at the web. Specimen #3 was designed for approximately 70% of the reduced moment capacity of the smaller section in splice and 25% of the reduced shear capacity. Since the holes reduce the area of the section, the nominal member capacity decreases at the splice location to about  $0.68M_p$  for all specimens. Connection component material was also tested.

### 2.1.1 Details and capacity estimation of specimens

The specimens were designed based on the model proposed in the Connection Design Guide 13 [8], which is in accordance with Australian Standard AS 4100 [8]. The model assumes that, for I section columns, the moment is carried through cover flange plates while the web plates transfer the shear force.

In this model, the capacity of bolts at flanges is determined based on the minimum value of shear capacity of bolt, local bearing capacity and end plate tear-out of flange and cover plate. The capacity of flange cover plate is determined by minimum of elastic capacity of gross area or plastic capacity of net area excluding the holes. The design shear capacity of the web cover plate,  $0.5f_y t_w d_w$ , is also required to be greater than the design shear action.  $f_y$ ,  $t_w$  and  $d_w$  are the yield stress, thickness and width of the web plate, respectively.

Flange splices are required to provide high stiffness at service levels. For the flange splice configuration of Specimens #1 and #2, slip is estimated to occur at  $0.24M_p$  assuming the friction coefficient is 0.35 for rolled steel surfaces, and tension per M20 bolt at installation (proof load) is 145kN without considering the capacity reduction factor, 0.7, at serviceability limit state [8]. Slip is predicted at  $0.36M_p$  for the flange splice configuration of Specimen #3.

Based on the design model, the specimens are expected to develop the following capacity for each component as listed in Table 1. All estimations are based on the reduced design capacities of the components. Table 2 shows specimen details.

Table 1 – Reduced design capacity of connections

Specimen	Design capacity of flange splice				Design capacity of web splice			
	Plate component		Bolt component		Plate component		Bolt component	
	Capacity	Failure mode	Capacity	Failure mode	Capacity	Failure mode	Capacity	Failure mode
#1	$0.5M_p$	Plasticity in the net area	$0.44 M_p$	Shear in bolt	$0.58V_y$	Shear failure	$0.34V_y$	Interaction of shear and induced moment
#2	$0.5M_p$	Plasticity in the net area	$0.44 M_p$	Shear in bolt	-	-	-	-
#3	$0.84M_p$	Plasticity in the net area	$0.67 M_p$	Shear in bolt	$0.58V_y$	Shear failure	$0.34V_y$	Interaction of shear and induced moment



Table 2 – Detail of the connections in moment tests

Specimen	Top and side views	Testing axis	Flange cover plate		Web cover plate		Flange bolts		Web bolts	
			Thickness	Grade	Thickness	Grade	Number	Grade	Number	Grade
#1		Major	12	300	6	350	32	8.8	4	8.8
#2		Major	12	300	-	-	32	8.8	-	-
#3		Major	20	300	6	350	48	8.8	4	8.8

### 2.1.2 Test Setup and loading regime

Fig.1 shows the moment configuration under the Dartec 10MN universal testing machine. The Dartec upper portion is supported by four columns (not shown in the figure). It may be fixed at any height and a hydraulic actuator at the bottom applies cyclic loading.

The top and bottom setup beams are attached to the Dartec by four 2" bolts of high strength steel Grade 4140. While the bottom beam moves with the actuator, the top beam is stationary. Special connections were designed to facilitate the cyclic loading. Each connection consists of a block accommodating a roller and threaded rods connecting a thick plate accommodating another roller on the other side of specimen. The rollers are restrained by edge plates which allow them to move horizontally but not vertically. The threaded rods are pulled enough to let the rollers rest on the specimen while avoiding pre-tensioning. Eight M24 bolts were used to connect the bottom of the blocks to the support beams.

When the actuator moves up, the end bottom rollers push up the specimen ends and the middle top rollers apply downward force on the specimen. When the actuator moves down, the forces are applied in the opposite direction through the opposite rollers. In this state, the threaded rods are activated in tension to transfer the forces.

The setup provides constant moment between the loading points without significant shear force. The displacement of the specimen was measured at four bearing points as well as the center to provide the deformation profile of the specimen.

Although the right end rollers were prevented from rolling, the specimen could slide on them under heavy loads. As such, a link was fabricated to stop the horizontal movement of the specimen while allowing the rotation.

The loading in this study is controlled by the displacement of the Dartec actuator. Since the bolts attaching the setup to the Dartec could not be post-tensioned due to the large diameter, they experienced slackness in tension. This was observed as high as 0.8mm at the bottom connection for about 2000kN force of the Dartec. Therefore, the input displacement on the specimen is less in tension than in compression. The loading regime applied in the experiments is shown in Figure 2.

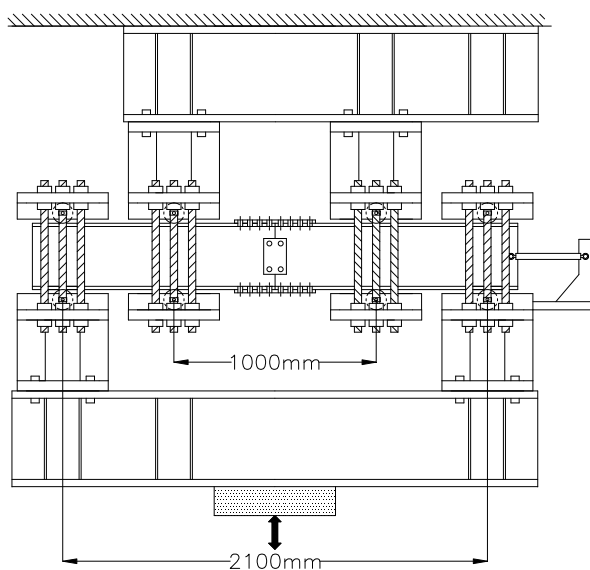


Figure 1 – Test setup

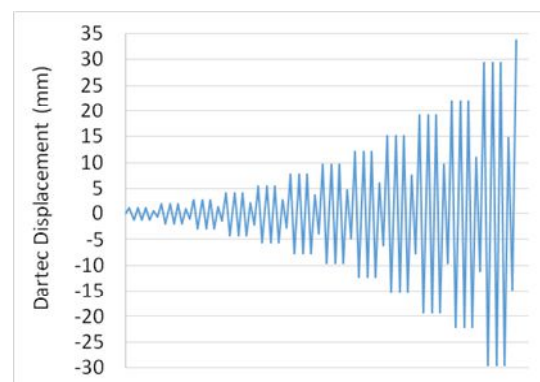


Figure 2 – Loading regime

### 2.1.3 Instrumentation

String potentiometers were used to measure the absolute displacement of the beam at the ends and in the middle of the specimen. The two mid-loading points in this setup are constrained between the top and bottom rollers which are both fixed. Two linear potentiometers were attached to the top and bottom flanges to measure the gap between the spliced sections. The data provides the displacement profile of the beam and the splice rotation at each load step. Fig. 3 shows a typical example of using linear potentiometers installed on the specimen. Other instrumentation devices seen in the photo are not the subject of this study.



Figure 3 – Instrumentation of the connection

### 2.2 Model

Numerical analyses of the splice connections were carried out to predict their moment-deformation behavior. Three equations were developed of which one is the compatibility of deformations at the section and two others are the equilibrium of the section axial forces and their moment about the neutral axis. Fig. 4 shows the schematic forces acting on the sections before compressive stresses reach their yield. These two halves shown separated for clarity are actually in contact. The stresses are shown to increase linearly with distance from the neutral axis. At large rotations, the yield strength of some components will be reached and the stress distribution will become trapezoidal. Since the moment over the central region of the beam, where the connection is placed is constant, the deformation at the exterior of the flange on the compressive side of the connection,  $\Delta_c$ , can be expressed by Eq. (1) where  $L_{connection}$  is the distance between the farthest bolt to the centre of the connection. The deformation at the level of the outside of the flange on the tensile side of the connection is given by  $\Delta_t$ , which consists the axial deformation of the splice plate, shear deformation of the bolts and ovalization of the bolt holes. The compatibility of compressive and tensile deformations is expressed in Eq. (2). The force displacement model used to characterize the behavior of the splice plate in tension is as Eq. (3). The form of the equation was initially developed by Fisher, while the values of the coefficients were later determined by Crawford and Kulak based on six single bolt shear tests [9]. This equation is very general and does not consider parameters such as bolt diameter and length, failure mode, packer plates and the thicknesses of the plates [9]. The maximum predicted displacement is based on the ultimate shear capacity of the bolts.

In this study, it was assumed that the compressive stresses are transferred through the splice plate in compression and the contact area of the section. The tensile force is considered to be the sum of bolt shear forces. Bolt shear in the compression side of the splice was ignored in the equations, but the splice plate and flange on the compression side were assumed to behave compositely here. Also, prying actions, in particular due to splice plates, were not modeled here.

$$\Delta_c = \frac{\sigma \times L_{connection}}{E} \quad (1)$$

$$\frac{\Delta_c}{\Delta_t} = \frac{x}{h-x} \quad (2)$$

$$F_t = n_{bolt} \times F_{ult} \times (1 - e^{-0.394\Delta_t})^{0.55} \quad (3)$$

For simplicity, the slippage due to over-size holes was ignored in the equations. Initially the bolts were assumed to be centered in the holes. The slippage due to oversize holes is associated with a rotation of the sections about 0.012 radians ( $2 \times 2(\text{mm})/d$ ), where  $d$  is the distance between inner sides of the splice plates. The deformation of the connection was later increased by the slippage deformation at the predicted slip force. Web splices were not considered in the model.

Ultimate strength of bolts in shear ( $F_{ult}$ ), and yield stress of the flanges and plates were considered to be 137kN and 300MPa respectively. These values are the average results from the sample material tests.

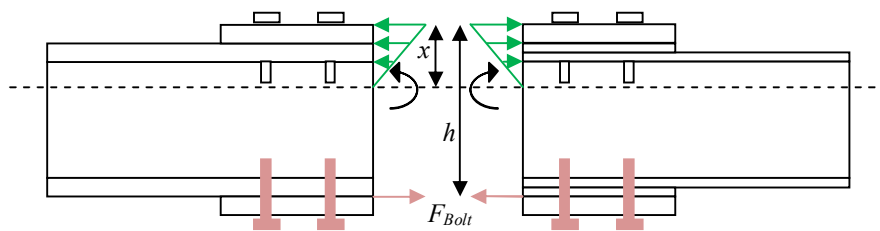


Figure 4 – Schematic forces acting on the bearing splice sections

### 3. Results and Discussion

#### 3.1 Specimen #1 – 50% strength with web plate

The specimen consists of two wide flange sections, 310UC158 and 310UC118. The dimensional difference of the sections is 12mm which is filled by two 6mm filler plates on each side. High strength zinc-plated bolts, threaded over all their length, were used to connect the flange splice plates. The web bolts were partly threaded from the same material.

The bolts were snug-tightened with a hand torque wrench set to apply 145N.m. This was less than the torque recommended by the fabrication company to obtain approximately 65% of the proof load, which was 372Nm. The likely axial force was therefore about 65% x (145kNm/372kNm) x PROOF LOAD (145 kN) x  $N$  bolts = 65% x 145kNm/372kNm x 145kN x 8 bolts = 294kN. The friction force, assuming a coefficient of 0.25, which is less than the standard value of 0.35 from NZS3404 for a cleaned connection, is 74kN. This value is used because the contact surfaces were contaminated with drilling oil and loose particles, resulting in a smaller initial slip force. The associated moment predicted from the flange bolts is 74kN x 0.327m = 24 kNm, which is only 4.5% $M_p$ .

With bearing between the compression flange ends, the expected slip all occurs on the tension side. If the bolts are centered in the 2mm oversize holes, then the rotation anticipated before bolt bearing occurs is approximately 4mm/327mm = 0.012% due to the holes either side of the splice, and there being 2 holes that each bolt passed through assuming the bolts remain vertical.

Figure 5 shows that the actual slope before load increased significantly was about 0.02 radians or 2%. This is likely to be as a result of the bolts rotating and possibly not being perfectly centered as well as a small fabrication gap (0.5 mm) between the spliced members. The actual strength before the bolts started increasing strength due to bearing was less than 0.1 $M_p$ . This is consistent with the low predicted strength of 4.5% $M_p$ .

The design strength was 0.44 $M_p$  for the bolts and 0.50 $M_p$  for the plates from Table 1. Of these, the bolts control the splice design strength as they are weaker. The predicted strength at large rotations using the equations

above was  $0.65M_p$ . The peak strength measured was about  $0.75M_p$  as shown in Figure 5. This is about 50% greater than the  $50%M_p$  considered in the design for the plates, and 70% greater than the  $44%M_p$  considered in the design for the bolts. The model based on Equations 1-3 seemed to represent the overall behavior envelope well.

It can also be seen that the loops corresponding to the second and third cycles after the slippage show slackness and gapping due to hole elongation. The maximum elongation in the splice plates and the shear deformation in the bolts were approximately 4mm and 5mm, which allows a  $2 \times 9\text{mm}/327\text{mm} = 0.055\%$  displacement after slippage. This is consistent with the post-slippage displacement of about 6% seen in Figure 5.

The bolts on the bottom splice plate of the smaller member failed in shear and the bolts were projected out with very high speed as an explosion. This occurred as the elastic flexural energy in the splice plates was released as the bolts failed. While the bending/prying of the splice plates on the tension side puts tension on the bolts, this did not seem to adversely affect the splice flexural strength.

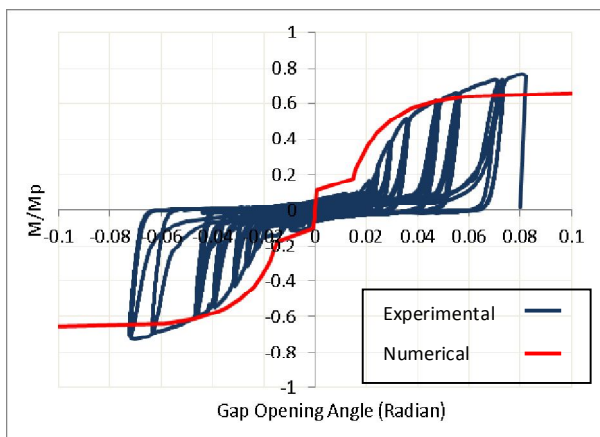


Figure 5 – Hysteresis behavior of Specimen #1

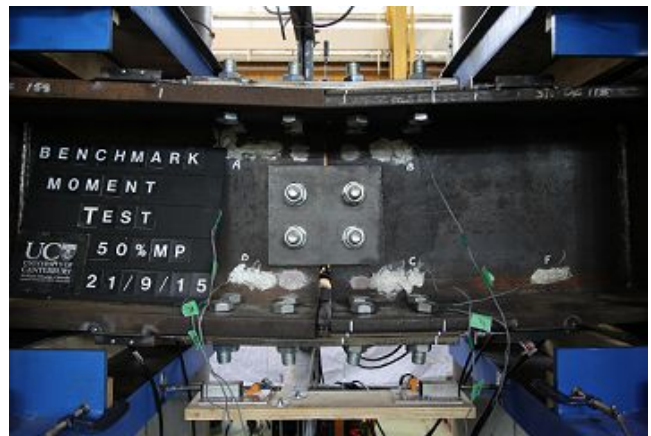


Figure 6 – Rotation of Specimen#1 close to failure

Fig. 7 shows the damage in the splice plate. It is seen that all the holes yielded in bearing and the plate yielded along the inner row of the bolt holes. Also, it is clear that hole ovalization is larger for the inner rows compared to the edge rows. The average elongation was observed to be 3.9 mm and 1.3 mm for inner and edge rows, respectively. Fig. 8 shows the damage in the web holes. Although it is assumed that web splices do not contribute in transferring bending moment, they could damage in large rotations which could potentially affect their shear performance.

Fig. 9 shows the distortion of the flange at the location of splice is approximately 1 mm. Fig. 10 shows the separation of the splice plate and the packer close to the connection failure. The damage could be attributed to prying actions and piled up material behind the bolts.



Fig. 7 – Damage in flange splice plate



Fig. 8 – Damage of the web in 310UC118 section



Fig. 9 – Damage in the flange of the smaller section



Fig. 10 – Gap between the connection plates

### 3.2 Specimen #2 – 50% strength with no web plate

Unlike Specimen 1, the contact surfaces were prepared before fabricating the specimen. The surfaces were cleaned with a wire brush to remove the loose mill scale and then wiped with solvent to remove any contamination with drill oil. The bolts were proof tightened with 1/3 of a full turn as recommended by manufacturers to obtain 145kN tension in bolts. This was more tightening than that for bolts in Specimen #1.

Fig. 11 shows the hysteresis behavior of the connection. Initially, the friction force in this case is about  $0.2M_p$  which is very close to the estimated value calculated as follows. The friction force, assuming a coefficient of 0.35, is  $0.35 \times 145\text{kN} \times 8 \text{ bolts} = 406\text{kN}$ . The associated moment from the flange bolts is  $406\text{kN} \times 0.327\text{m} = 133 \text{ kNm}$ , which is equal to  $24\%M_p$ .

The slip force is greater than that of Specimen #1 due to the different construction. However, it can be observed that the friction force reduced in the larger displacement cycles. The connection rotational capacity is 0.084 radians which is 5% more than that of Specimen #1. The ultimate strength is approximately  $0.75M_p$  which is similar to that of Specimen #1. Also, Specimen #2 is more flexible at larger rotations than Specimen #1 which is likely to be as a result of the absence of web splice. The failure mode was the same as Specimen #1 with sudden explosion.

The numerical model shown with the red line in Fig. 11 is identical to that of Specimen #1 as the web plate effect was ignored in the model.

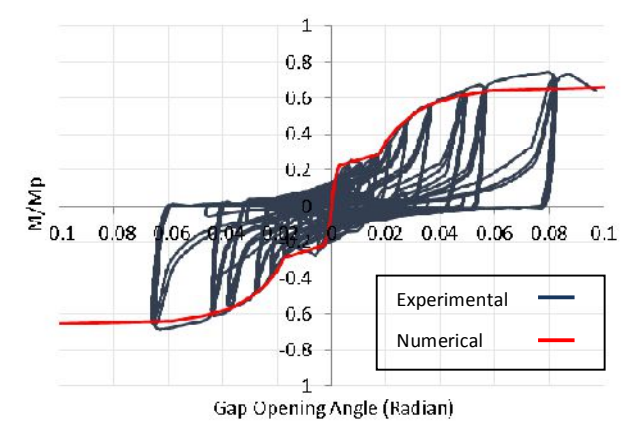


Fig. 11 – Hysteresis behavior of Specimen #2

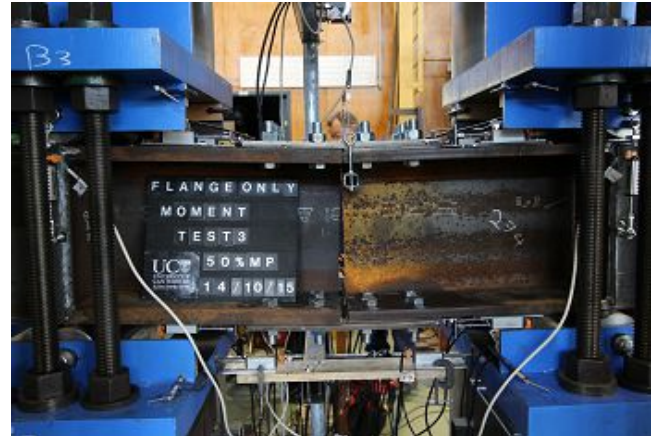


Fig. 12 – Specimen #2

Fig. 13 and 14 show the damage in the splice plate and the flange of the smaller member. The inner rows of the holes in the splice plate elongated 2.7mm on average, but no elongation was observed for the edge rows. Fig. 15 shows the extent of deformation in a bolt at its failure.



Fig. 13 – Damage in flange splice plate



Fig. 14 – Damage of the flange in 310UC118 section

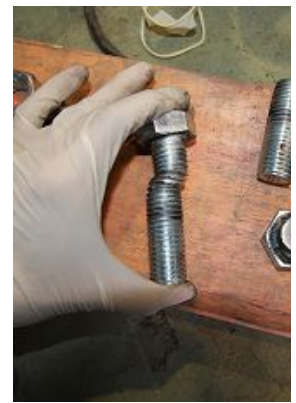


Fig. 15 – Bolt deformation

### 3.3 Specimen #3 – 70% strength with web plate

The contact surfaces were cleaned as in Specimen #2 preparation. The bolts were tightened to 1/3 of a turn from the snug-tight condition.

The cyclic performance of the connection is illustrated in Fig. 16. The predicted slippage strength of about  $0.32M_p$  is larger than  $0.22-0.28M_p$  observed. The connection ultimate strength capacity is greater than  $M_p$  even though holes were present in the flange and beam. This could be attributed to flange strain hardening as well as to the splice plate. Also, the connection exhibits larger stiffness compared to the other two specimens. The connection has smaller rotational capacity compared to the other two specimens possibly because the thicker (20mm) flange splice plate was stronger and had less bolt hole deformation under the forces imposed by the bolts.

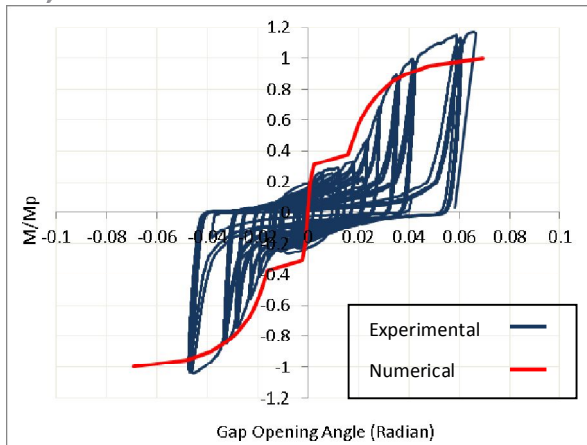


Fig. 16 – Hysteresis behavior of Specimen #3



Fig. 17– Specimen #3

Beam flange and web damage was larger than in Specimens #1 and #2. The 6mm web plate material is of Grade 350 rather than the Grade 300 11.9mm thick beam web. Interestingly, the web plates were damaged less than the web itself. Figs. 18 and 19 show the damage in the smaller member. No significant elongation was observed in the splice plate holes. The same failure mode was observed in the test as in the other two tests.



Fig. 18 –Damage of the flange in 310UC118 section



Fig. 19 –Damage of the web in 310UC118 section

#### 4. Conclusions

The paper describes three cyclic flexural experiments on bolted wide flange member splices. It was shown that:

1. In all the experiments, connections developed about 50% larger strengths than their reduced design capacities. The friction force effect diminished in larger cycles regardless of the initial friction force. The hysteretic behavior followed that of a gapping system due to hole elongation. This elongation was greater for bolts closer to the centre is of the section.
2. The effect of the web splice on flexural performance was negligible in this study where the member was subject to pure flexure with no shear. However, damage was observed in the web when web plates existed. While modifying the slip surface and increasing the bolt tightness increased the initial sliding strength, it had no significant effect on the total strength.
3. A simple approach to estimate the behavior of splice connections was developed and verified by the experimental results.

## 5. Acknowledgements

The authors would like to acknowledge the staff of the University of Canterbury Structural Engineering Laboratory for their assistance to conduct the experiments, The Natural Hazards Research Platform for the financial support of this PhD research, and John Jones Steel NZ for constructing the experimental setup. Also, they acknowledge the sponsorship from Opus International Consultants Ltd, Auckland, New Zealand of the paper registration at 16WCEE.

## 6. References

- [1] AISC (2010): *Seismic Provisions for Steel Structural Buildings, AISC 341-10*, American Institute of Steel Construction. Chicago, IL.
- [2] NZS3404 (1997): *Steel structures standard*. Part1. New Zealand.
- [3] Bruneau, M, Mahin SA (1990): Ultimate Behavior of Heavy Steel Section Welded Splices and Design Implications, *Journal of Structural Engineering*, **116**(8): 2214–2235.
- [4] Stillmaker K, Kanvinde A, Galasso C(2015): Fracture Mechanics-Based Design of Column Splices with Partial Joint Penetration Welds. *J. Struct. Eng.*
- [5] Edwards JH, Whittemore HL, Stang AH (1929): Transverse tests of H-section column splices. *Bureau of Standards Journal of Research*, **4**(3), 395–413
- [6] Douty RT, McGuire W(1965): High Strength Bolted Moment Connections. *Journal of structural Division*, 91.
- [7] Beedle LS, Christopher R (1963): Tests of steel Moment Connections. *Structural Engineers Association Proceedings*.
- [8] Hogan TJ, Van der Kreek N (2009): Connection Design Guide 13. RIGID CONNECTIONS.
- [9] BJORHOVDE R, COLSON A, ZANDONINI R (1996): Connection in Steel Structures III: Behaviour, strength and Design